AD-A093 268 IBM THOMAS J WATSON RESEARCH CENTER YORKTOWN HEIGHTS NY F/6 7/3
THE VIBRATIONS AND STRUCTURE OF PYRIDINE CHEMISORBED ON AG(111)--ETC(U)
NOV 80 J E DEMUTH, K CHRISTMANN, P N SANDA N00014-77-C-0366
UNCLASSIFIED TR-11 NL

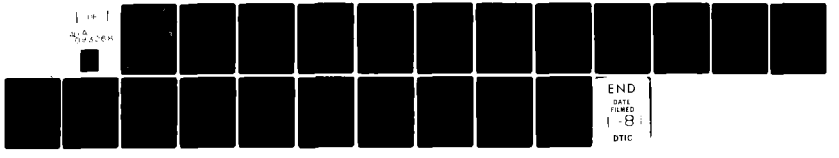

END
DATE FILMED
8
DTIC

LEVEL

OFFICE OF NAVAL RESEARCH

Contract N00014-77-C-0366

Task No. NR 056-123

TECHNICAL REPORT NO.11

The Vibrations and Structure of Pyridine Chemisorbed on Ag(111): the Occurrence of a Compressional Phase Transformation

by

J.E. Demuth, K. Christmann

and P. N. Sanda

Prepared for Publication

in

Chemical Physics Letters

IBM T.J. Watson Research Center

Yorktown Heights, NY 10598

November 21, 1980

UNCLASSIFIED

SECURITY CLASSIFICATION OF THIS PAGE (When Data Entered)

REPORT DOCUMENTATION PAGE		READ INSTRUCTIONS BEFORE COMPLETING FORM
1. REPORT NUMBER: Technical Report, No. 11	2. GOVT ACCESSION NO.: AD-A093	3. RECIPIENT'S CATALOG NUMBER: 368
4. TITLE (and Subtitle): The Vibrations and Structure of Pyridine Chemisorbed on Ag(111): the Occurrence of a Compressional Phase Transformation.		5. TYPE OF REPORT & PERIOD COVERED
		6. PERFORMING ORG. REPORT NUMBER
7. AUTHOR(s): J.E. Demuth, K. Christmann, and P.N. Sanda		8. CONTRACT OR GRANT NUMBER(s): N00014-77-C-0366
9. PERFORMING ORGANIZATION NAME AND ADDRESS: IBM T.J. Watson Research Center, P.O. Box 218, Yorktown Heights, NY 10598		10. PROGRAM ELEMENT, PROJECT, TASK AREA & WORK UNIT NUMBERS
11. CONTROLLING OFFICE NAME AND ADDRESS: Office of Naval Research, Chemistry Program Office, Arlington, VA 22217		12. REPORT DATE: November 21, 1980
		13. NUMBER OF PAGES
14. MONITORING AGENCY NAME & ADDRESS (if different from Controlling Office)		15. SECURITY CLASS. (of this report): Unclassified
		15a. DECLASSIFICATION/DOWNGRADING SCHEDULE

16. DISTRIBUTION STATEMENT (of this Report)

Approved for Public Release; Distribution Unlimited.

17. DISTRIBUTION STATEMENT (of the abstract entered in Block 20, if different from Report)

18. SUPPLEMENTARY NOTES

To appear in Chemical Physics Letters

19. KEY WORDS (Continue on reverse side if necessary and identify by block number)

Surface, Chemisorption, Vibrations, structure, Pyridine, Bonding, Compressional phase transformation, Silver

20. ABSTRACT (Continue on reverse side if necessary and identify by block number)

High resolution electron energy loss and UV photoemission spectroscopies have been used to study the chemisorption of pyridine on clean Ag(111) at T~140K. Pyridine is weakly chemisorbed and undergoes a compressional phase transformation from a π-bonded species to a more weakly bound, nitorgen-lone-pair bonded species. The molecular orientations of both chemisorbed phases are determined.

DD FORM 1 JAN 73 1473

UNCLASSIFIED

SECURITY CLASSIFICATION OF THIS PAGE (When Data Entered)

The Vibrations and Structure of Pyridine Chemisorbed on Ag(111): the Occurrence of a Compressional Phase Transformation†

J.E. Demuth, K. Christmann,* and P.N. Sanda**

IBM T.J. Watson Research Center
Yorktown Heights, New York 10598

Abstract: High resolution electron energy loss and UV photoemission spectroscopies have been used to study the chemisorption of pyridine on clean Ag(111) at T ~ 140 K. Pyridine is weakly chemisorbed and undergoes a compressional phase transformation from a π-bonded species to a more weakly bound, nitrogen-lone-pair bonded species. The molecular orientations of both chemisorbed phases are determined.

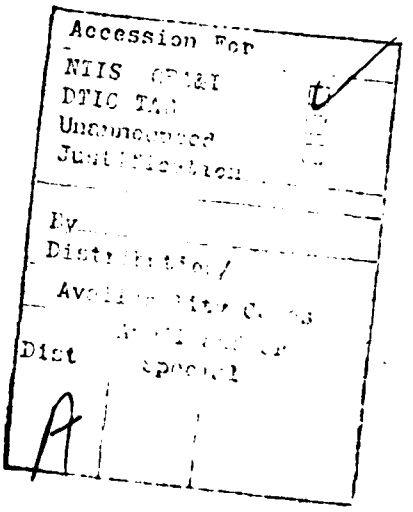

† Supported in part by the U.S Office of Naval Research.

* Permanent address: Institut für Physikalische Chemie der Universität München, W. Germany.

** Affiliated with Cornell University, Ithaca, NY 14850

Here we report high-resolution, electron energy loss (EELS), UV-photoemission (UPS) and thermal desorption spectroscopic (TDS) results for pyridine chemisorbed on a clean Ag(111) surface from which we determine its molecular vibrations as well as its orientation on the surface. We find that pyridine exhibits reversible, weak chemisorption on Ag(111) and is π-bonded for coverages up to 3 x 10^{14} molecules/cm^2. Increased coverage leads to a structural phase transformation where nitrogen-lone-pair bonding occurs and the molecule becomes inclined (~ 55°) to the surface and rotated (~ 30°) about the molecular C_{2V} symmetry axis. This compressed structure is more weakly bound to Ag(111) than the π-bonded phase and saturates at coverages of ~ 5 x 10^{14} molecules/cm^2. Such complex bonding and orientational effects have not been observed in previous studies of adsorbed pyridine [1-3] and are important for understanding the nature of surface enhanced Raman scattering for pyridine on Ag as observed in electrochemical [4] and ultra-high vacuum studies [5].

The experimental measurements were performed in two separate ultra-high vacuum (UHV) systems (pressure < 1 x 10^{-10} Torr). The first (turbo-molecular pumped) system described elsewhere [6] allows UPS, low-energy electron diffraction (LEED), Auger (AES) and TDS to be performed while the second (ion- and titanium-sublimator-pumped) system permits EELS and work function change measurements. The electron optics for EELS consists of two sets of 2.5 cm hemispherical deflection analyzers with associated focusing optical elements [7] so as to allow the monochromatization, reflection from a sample (total scattering angle of 90°) and energy analysis of a well-defined (< 0.2 mm dia.), collimated (<1°), low-energy (2-100 eV) electron beam. For the specular reflection of a 3 eV beam off of Ag(111), we have routinely obtained a total system resolution of 65-75 cm^{-1} (8-9 mV) with peak counting rates of 10^6 Hz. Although both the monochromator and analyzer are in fixed position, the sample rotation is

arranged so as to enable the observation of specular ($\theta_{in} = \theta_{out}$) as well as off-specular ($\theta_{in} \neq \theta_{out}$) scattering events in the plane of incidence.

The Ag(111) surface was prepared by standard mechanical [6] and chemical polishing [8], then annealed and sputter cleaned as determined by AES. This clean, well-ordered Ag(111) sample was then inserted into the EELS system where further sputter cleaning and annealing was performed. Work-function change measurements performed in both UHV systems as well as EELS spectra served to verify surface cleanliness in the HREEL system. The final clean samples were mirror smooth and showed minimal optical defects or irregularities. All chemisorption experiments in the EELS system were done at temperatures of ~ 140K as monitored by a chromel-alumel thermocouple. UPS measurements were performed at temperatures down to 80 K.

Reagent grade pyridine (99.9%) and d_5-pyridine (99 atom % D) were used in these experiments. Sample dosing was done via the chamber ambient and directly monitored with an ion gauge. (All exposures cited here are in Langmuires, L ($1L = 10^6$ Torr-sec) and have been corrected by a gauge factor of 5.8 [9].) The dosages required to produce both the compressional phase and first physisorbed layers were identical in both UHV systems.

Our results indicate that a structural phase transformation occurs for chemisorbed pyridine on Ag(111) at an exposure of ~ 0.5L. In Fig.1 we show the EELS vibrational loss spectra of d_5-pyridine before (solid line) and after (dotted line) this transition. Here, the relative intensities of the CH deformation modes between 360-820 cm^{-1} strongly change, especially when compared to the relative IR-absorbances [10,11] also shown in Fig.1. This transition is more striking for normal pyridine C_5H_5N as shown in Fig. 2 for the chemisorption regime (< 1L exposure). For normal pyridine the

CH deformation modes at ~ 600 and 700 cm are clearly separated. Also, the strong decrease in intensity of the ~ 700 cm^{-1} feature above 0.5 L exposure indicates that at least 93% of the lower coverage phase converts to a new structure. The vibrational frequencies for both phases are identical within our experimental uncertainties of ± 5 cm^{-1}.

In order to obtain structural information from the loss spectra of chemisorbed pyridine on Ag(111), we must assign the observed vibrations. At the onset such an assignment would seem formidable based upon the relatively poor resolution of EELS and the fact that pyridine is of low symmetry and has 27 IR-active modes [12]. Fortunately, we find that we can straight forwardly assign most all the observed vibrational losses since (a) only a fraction of the 27 free-molecule modes have significant dipole scattering cross sections (i.e., IR absorbances [10,11], see Fig.1) and (b) all the vibrations we observe are weakly perturbed ($\Delta\nu_{avg}$ = ± 6 cm^{-1}) relative to liquid pyridine. In Table I, we list the observed vibrational losses for normal and deuterated pyridine as well as the vibrations for liquid pyridine with absorbances, A greater than ~ 1% of the largest value [10,11]. The symmetry class and mode number as designated by Long and Thomas [12] are also indicated. Comparisons between normal and deuterated pyridine as well as the corresponding relative intensities help in our identification and assignments. We also interpret the 700 cm^{-1} loss for low coverages of deuterated pyridine as a combination band of ν_{26} and the pyridine-metal-stretching vibration (PM) since ν_{26} is very intense and has a symmetry which will allow coupling. The resulting (deuterated) pyridine-metal vibration of ~ 175 cm^{-1} is also in agreement with that observed for normal pyridine (~ 200 cm^{-1}) and observed in other pyridine-metal compounds [13]. Interestingly, we see no evidence for the presence of ν_{25} , a rather strong IR mode but which has extremely asymmetric deformation motions. This is true for ν_{17} which is also not observed. Finally, we cannot assign

(a) which CH-stretching modes we observe due to our limited resolution, nor (b) the character of the 1220 or 1570 cm^{-1} losses for normal pyridine. Fortunately, these last ambiguities play no role in our structural analysis.

From our assignments in Table I, the observed coverage-dependent changes in the loss spectra of Fig.2 near ~ 0.5 L are associated with a reduction in the intensity of the out-of-plane CH-deformation modes at ~ 400 and 705 cm^{-1} and an increase in the in-plane CH-deformation mode near 610 cm^{-1} (and similarly for d_5-pyridine in Fig.1). By comparing the relative intensities of these in-plane and out-of-plane modes and relating them to the "structurally-averaged" dipole-scattering intensities (i.e., IR-absorbances) of liquid pyridine, we can determine the molecular orientation. Here, we exploit the dipole-scattering mechanism for *specular* electron scattering [14] and assume the surface selection rule that only the normal components of these modes will be observed in EELS [15]. For pyridine inclined at an angle θ to the surface, the loss intensities for in-plane (I_{in}) and out-of-plane (I_{out}) deformation modes are related by

$$\frac{A_{in}}{A_{out}} \tan \theta = \frac{I_{in}}{I_{out}},$$

where A is the IR absorbance and we assume a constant transmission function for our spectrometer [16]. Applying this relation to the out-of-plane deformation modes ν_{26} and ν_{27} and the in-plane deformation mode ν_{10} we determine averaged angles of ~ $5\pm3^\circ$ at low coverages (< 0.4 L) and ~ $57\pm3^\circ$ at higher coverages (0.6-0.8 L). For these higher coverages we have assumed that the structural conversion is complete. This assumption turns out to be consistent with the resulting geometry which provides (a) the correct relative saturation coverages of both phases and (b) the proposed intermolecular stabilization mechanism as discussed later. Based upon our UPS results (to be described) as well as other chemical arguments

and results [1,2], this strongly-inclined phase has the nitrogen end of the molecule directed into the surface.

For exposures above 0.5 L we also find another in-plane deformation mode at 1440 cm^{-1} (1305 cm^{-1}, d_5-pyridine) which also becomes EELS active. This mode turns out to have net motions almost completely perpendicular to the C_{2v} symmetry plane of the molecule. Again, considering the surface-selection rule [15], leads us to conclude that the molecule is rotated about the C_{2v} symmetry axis. Applying the aforementioned intensity analysis to ν_{10} and ν_{14} gives rotational angles of 24° and 40° for normal and deuterated pyridine, respectively. These rotations also change the determined angles of inclination, but only slightly, to 53° and 48° respectively, since ν_{10} has little net motions parallel to the C_{2v} symmetry axis. This leads us to estimate a rotational angle of ~ 30° and an inclination angle of 55° ± 5°, respectively. From our off-specular scattering data, we have also estimated an upper limit for non-dipole scattering which does not significantly alter these values.. However, we have excluded the losses at ~ 1000 and 1570 cm^{-1} for normal pyridine (and the corresponding losses for deuterated pyridine) in our intensity analysis as they appear to have strong contributions from non-dipole scattering [17].

Our UPS spectra ($h\nu$ = 21.2 eV) are also consistent with a coverage-dependent reorientation of pyridine on Ag(111). In Fig.3 we summarize difference spectra obtained in the low and high coverage regimes of chemisorbed pyridine as well as for condensed pyridine and gaseous pyridine [18]. Here, we show only the orbitals which correspond to gas phase ionization potentials of less than 12 eV since the higher-lying (π_2,π_3,n) orbitals of chemisorbed pyridine overlap the Ag(111) d-band emission and cannot be resolved with certainty. The character of the ground-state orbital(s) associated with each ionization level is labeled [19] according to the level ordering [20]. The overall displacement in level positions (dotted

lines in Fig.3) for exposures above 1 L is associated with differences in relaxation and initial state polarization shifts for condensed versus chemisorbed species and indicates that all pyridine below this exposure *must be* chemisorbed [21]. After considering a uniform relaxation shift [21], the ionization levels of condensed and gaseous pyridine are nearly identical whereas chemisorbed pyridine shows differences in the relative positions of the high-lying levels. Namely, the low-coverage phase does not show the π_1 level which can be shifted to lower energies for a π-bonded species [21] so as to overlap with the σ_{cc},"n" and σ_{cc} levels. For higher coverages after the phase transformation, the π_1 level is observed and the level having nitrogen-lone-pair character (σ_{cc},"n") is perturbed and shifted to lower binding energies. This level is expected to shift if the high-lying nitrogen-lone-pair orbital becomes involved in bonding [22,23].

In Fig.4a and b, we schematically show the bonding orientation of chemisorbed pyridine at low and high coverages and propose a brief phenomenological description of the phase transformation. At low coverages pyridine bonds through the π-orbitals where an additional interaction of the surface via the nitrogen-lone-pair orbital may account for the small initial inclination. As this π-bonded phase approaches saturation coverage, we find that the sticking coefficient drops to almost half its initial value (as determined from UPS versus exposure data) and retains this value even when condensation occurs. Although we see no LEED patterns for any stage of chemisorption [24], a dramatic increase occurs in the electron reflectivity nearing completion of the π-bonded phase. Such phenomena in EELS is generally observed when well-ordered superstructures form [25,26]. We thus believe that a nearly-ideal close-packed ordered array of π-bonded pyridine occurs; and assuming a close-packed but commensurate pyridine monolayer, we estimate it to have a packing density of 3×10^{14} molecules/cm^2. Continued exposure allows additional molecules to squeeze

into defects or irregularities in the pyridine overlayer causing adjacent domains of molecules to become inclined. The resulting increased packing density produces more space on the surface and allows for island growth of this compressed structure. From the relative coverages determined by UPS, we estimate a density of 5×10^{14} molecules/cm^2 for this compressed phase prior to condensation. This compressional phase transformation is also reversible, and from thermal desorption results, we estimate that it is ~ 2 kcal/mode less strongly bound to the surface than the π-bonded phase.

Although we find π-bonded pyridine to be more strongly bound to Ag(111) than nitrogen-lone-pair bonded pyridine, the latter becomes preferred in the compressed phase. The loss of binding energy upon reorientation of π-bonded pyridine can be regained from intermolecular interactions. Given the aforementioned relative packing densities and our determined angle of inclination for the compressed phase, an attractive π_3-nitrogen-lone-pair interaction may occur (see Fig.4b). Such an interaction is reasonable since these orbitals are nearly degenerate. This interaction also accounts for the determined molecular rotation since the π_3 orbital phasing [19] is such as to allow only one side of the molecule to interact with the nitrogen-lone-pair orbital of an adjacent molecule.

In summary, we present evidence that pyridine π-bonds to the Ag(111) surface until it goes through a compressional phase transformation where it then bonds to the surface via the nitrogen-lone-pair orbital.

References

[1.] B.J. Bandy, D.R. Lloyd and N.V. Richardson, Surface Sci. **89** (1979) 344.

[2.] F.P. Netzer, E. Bertel and J.A.D. Matthew, Surface Sci. **92** (1980) 43.

[3.] S.R. Kelemen and A. Kaldor, Chem. Phys. Lett. **73** (1980) 205.

[4.] M. Fleischmann, P.J. Hendra and A.J. McQuillan, Chem. Phys. Lett. **26** (1974) 163; D.L. Jeanmaire and R.P. Van Duyne, J. Electroanal. Chem. **84** (1977) 1; M.G. Albrecht and J.A. Creighton, J. Amer. Chem. Soc. **99**, (1977) 5215.

[5.] R.R. Smardzewski, R.J. Colton and J.S. Murday, Chem. Phys. Lett. **68** (1979) 53; J.E. Rowe, C.V. Shank, D.A. Zwemer and C.A. Murray, Phys.Rev. Lett. **44** (1980) 1770; P.N. Sanda, J.M. Warlaumont, J.E. Demuth, J.C. Tsang, K. Christmann, and J.A. Bradley, to be published.

[6.] J.E. Demuth, Surf. Sci. **69** (1977) 365.

[7.] J.A. Simpson and C.E. Kuyatt, Rev. Sci. Inst. **38** (1967) 103.

[8.] H.J. Levinstein and W.H. Robinson, J. Appl. Phys. **33** (1962) 3149.

[9.] This corresponds to the guage-correction factor for benzene as supplied with our Varian ion guage.

[10.] L. Corrsin, B. Fox and R.C. Lord, J. Chem. Phys. **21** (1953) 1170.

[11.] D.J. Pouchart, *Aldrich Library of Infrared Spectra*, (Aldrich Chem. Co., Wisconsin, 1975).

[12.] D.A. Long and E.L. Thomas, Trans. Far. Soc. **59**, (1963) 783.

[13.] K. Nakamoto, *Infrared and Raman Spectra of Inorganic and Coordination Compounds,* (Wiley Interscience, NY, 1978) 211.

[14.] E.Evans and D.L. Mills, Phys. Rev. B **5** (1972) 4126.

[15.] D. Sokcevic, Z. Lenac, R. Brado and M. Sunjic. Z. Phys. B **28** (1977) 273.

[16.] This assumption is borne out by the narrow variation of inclination angles we determine in analyzing close-lying pairs of vibrations (i.e., ν_{27}/ν_{10} and ν_{26}/ν_{10}), but is more questionable when analyzing widely-separated features. The latter may account for the large variation found for the rotational angles.

[17.] Gas-phase electron-scattering work by I. Nenner and G.J. Schulz, J.Chem. Phys. **62**, (1975) 1747, shows strong vibrational excitations of *specifically* these two modes via temporary negative ion resonance scattering. This additional scattering contribution also explains why we see smaller than expected (dipole-derived) intensity variations with coverage for these two losses [see Fig.2].

[18.] D.W. Turner, et al: *Molecular Photoelectron Spectroscopy,* (Wiley Interscience, NY 1970).

[19.] W.L. Jorgensen and L. Salem, *The Organic Chemist's Book of Orbitals,* (Academic Press, NY, 1973) 263.

[20.] W. van Niesen, G.H.F. Diercksen and L.S. Cederbaum, Chem. Phys. **10** (1975) 345.

[21.] J.E. Demuth and D.E. Eastman, Phys Rev B **13** (1976) 1523.

[22.] J.E. Demuth, Phys. Rev. Lett. **40** (1978) 409.

[23.] H. Lüth, G.W. Rubloff and W.D. Grobman, Surf. Sci. **63** (1977) 325.

[24.] We use a conventional LEED display apparatus with ~ 10^{-6} Amp. beam currents which are well recognized to disrupt, desorb or disorder weakly adsorbed molecular species. (e.g., see J.C. Tracy, J. Chem. Phys. **56** [1972] 2736.)

[25.] H. Ibach, private communication

[26.] J.E. Demuth and H. Ibach, Surf. Sci. **85** (1979) 365.

TABLE I. Assignment of the observed vibrations for pyridine on Ag(111)

h_5-Pyridine			d_5-Pyridine			Sym.	Mode No.
on Ag(111)	IR(liquid)[10,11]		on Ag(111)	IR(liquid)[10,11]			
ν	ν	A	ν	ν	A		ν_P[12]
200	- - -	- - -	(175)	- - -	- - -	B_2	PM**
400	405	.55	365	371	.06	B_2	27
610	605	.63	560	582	1.77	A_1	10
705	700	1.39	525	530	.52	B_2	26
- -	- - -	- - -	700	- - -	- - -	B_2	26 + PM**
est 990	992	.99	965	962	.52	A_1	9
1040	1030	1.02	1020	1006	.05	A_1	8
	1068	.51	820	{823	.79	A_1	7
	942	<.02		823}		B_2	23
	{1218	.42	n-obs.	886	.11	A_1	6
1220	1218}	.42		908	<.02	B_1	16
1440	1439	1.71	1305	1301	1.77	B_1	14
	1482	.71		1340	<.02	A_1	5
1570	{1572	1.56	1540	{1542	1.43	B_1	13
	1583}	.87		1530}	1.20	A_1	4
	{3036	.41		{2285	.45*	B_1	12
	3036}			2254	.68	A_1	3
3040	{3055	.63	2260	{2293	.45*	A_1	1
	3055}			2270	.46	A_1	2
	{3083	.56		2290}	.45*	B_1	11
n-obs.	1148	.45	n-obs.	887	.11	B_1	17
n-obs.	749	1.30	n-obs.	567	<.02	B_2	25

* Overlapping bands.

* * Pyridine-metal-stretching frequency

Figure Captions

Fig.1. Vibrational loss spectra for 0.4 L (solid line) and 0.8 L (dotted line) exposures of d_5-pyridine to Ag(111). (The dashed line under the 0.6 L exposure spectra shows the spectrometer background signal at these magnifications). The IR-absorbances are compared to the loss spectra where we have shown all absorbances within 1% of the largest value [10,11]. (The absorbances denoted by * have been reduced by 1/3).

Fig.2. Vibrational loss spectra for pyridine between 350-1500 cm^{-1} as a function of exposure. The spectra shown at 2 x 10^{-7} Torr ambient pressures of pyridine corresponds to the onset of condensation, and the formation of the first physisorbed layer.

Fig.3. UV Photoemission difference spectra ($h\nu$=21.2 eV)(a) between the clean Ag(111) surface and a 0.35 L exposure to pyridine (the π-bonded phase) and (b) between a 0.52 L and 1.0 L exposure to pyridine (the nitrogen lone-pair bonded phase. A high exposure spectra for condensed (randomized) pyridine is shown in (c) which is compared to the gas phase ionization spectra [18]. All gaseous ionization features are derived from single orbitals except the second lowest feature which is derived from two orbitals [20].

Fig.4. Schematic diagram of the orientation and bonding of (a) the low coverage (< 0.4 L exposure) phase and (b) the high coverage (> 0.5 L exposure) compressional phase. Discrete bonding sites for pyridine on Ag(111) as well as pyridine's hydrogen atoms are not shown. In (b), the two molecules shown lie slightly below (right) and above (left) the plane of the page.

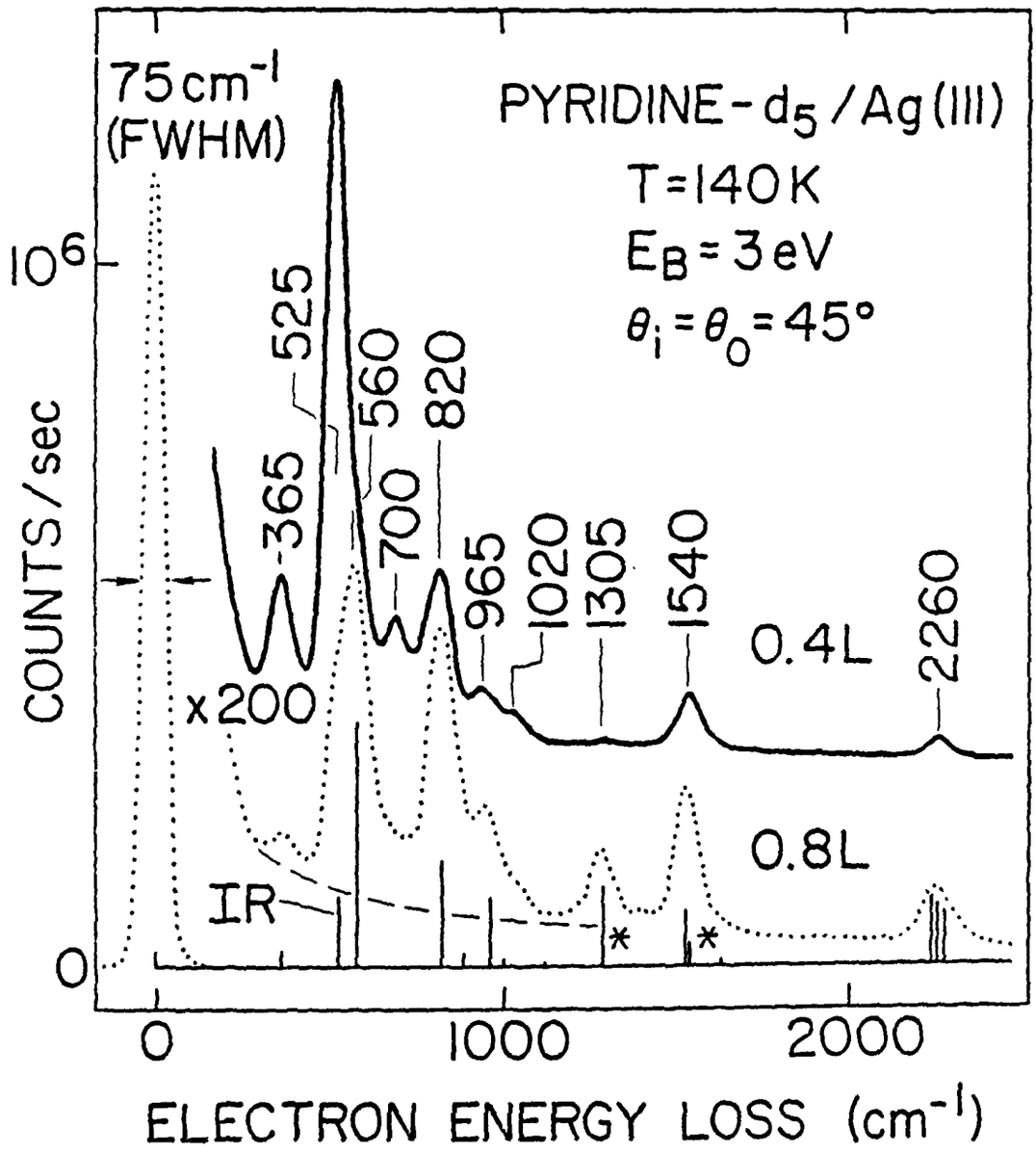
75 cm⁻¹
(FWHM)
PYRIDINE-d5 / Ag(111)
T=140K
EB=3eV
θi=θ0=45°
10⁶
0
COUNTS/sec
525
560
820
365
700
965
1020
1305
1540
2260
0.4L
x200
0.8L
IR
*
*
0
1000
2000
ELECTRON ENERGY LOSS (cm⁻¹)

FIG 1
DEMUTH

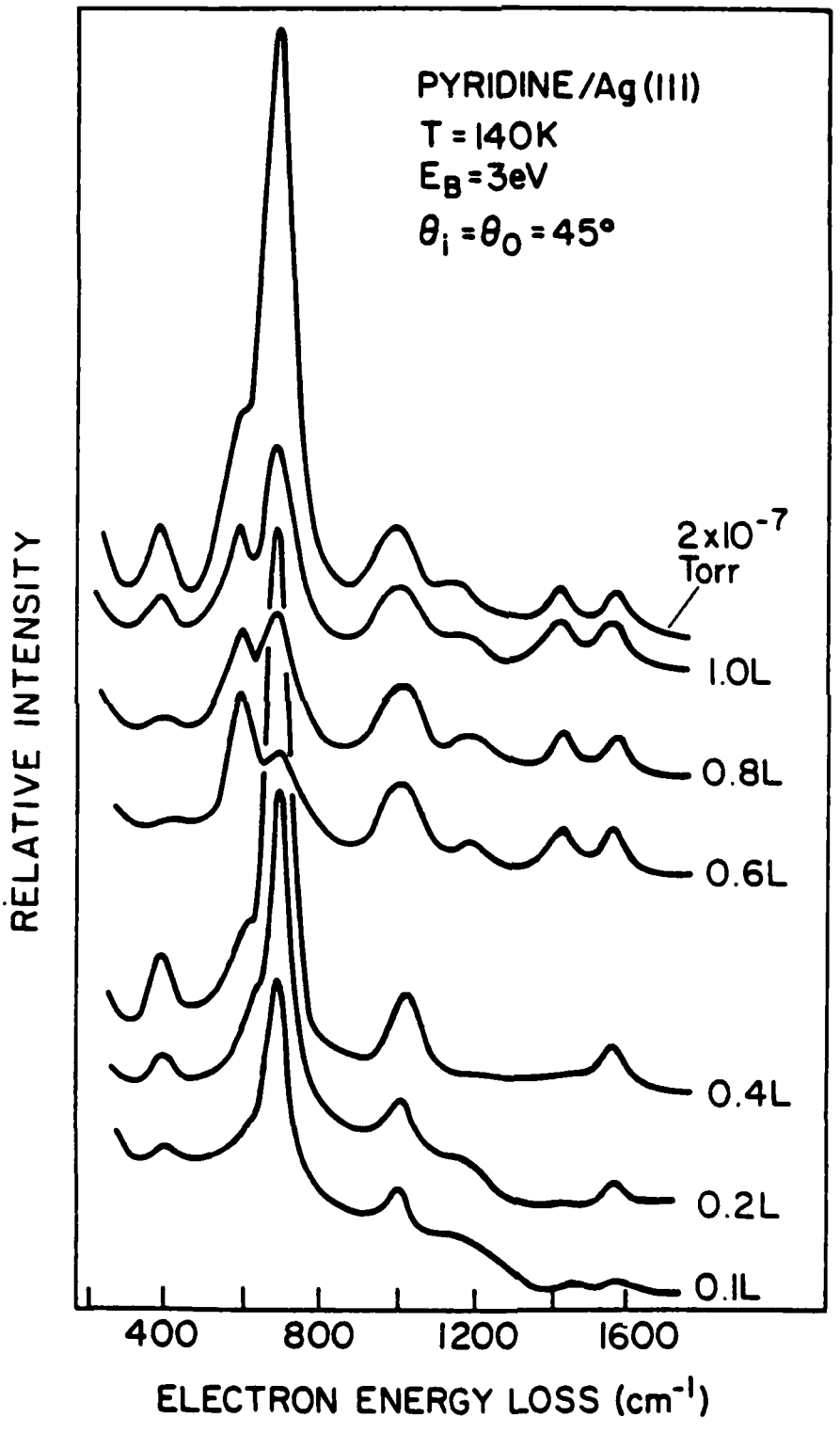
PYRIDINE/Ag(111)
T = 140K
E_B = 3eV
$\theta_i = \theta_0 = 45°$
2×10^{-7} Torr
1.0L
0.8L
0.6L
0.4L
0.2L
0.1L
RELATIVE INTENSITY
400
800
1200
1600
ELECTRON ENERGY LOSS (cm^{-1})

FIG 2

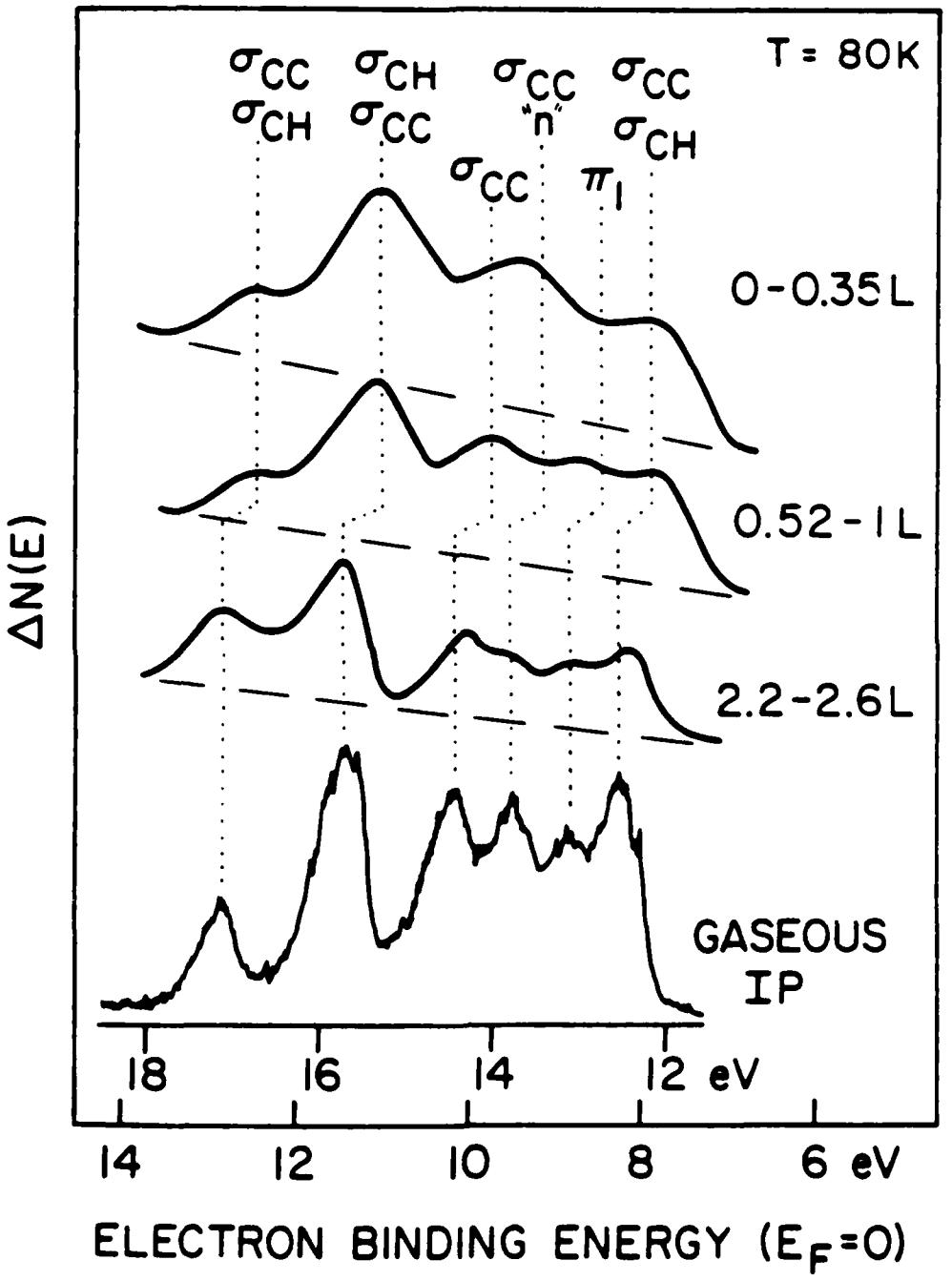
T = 80K
σ_{CC} σ_{CH}
σ_{CH} σ_{CC}
σ_{CC}
"n"
σ_{CC} σ_{CH}
π_1
0-0.35L
0.52-1L
2.2-2.6L
GASEOUS IP
ΔN(E)
18 16 14 12 eV
14 12 10 8 6 eV
ELECTRON BINDING ENERGY (E_F=0)

FIG 3

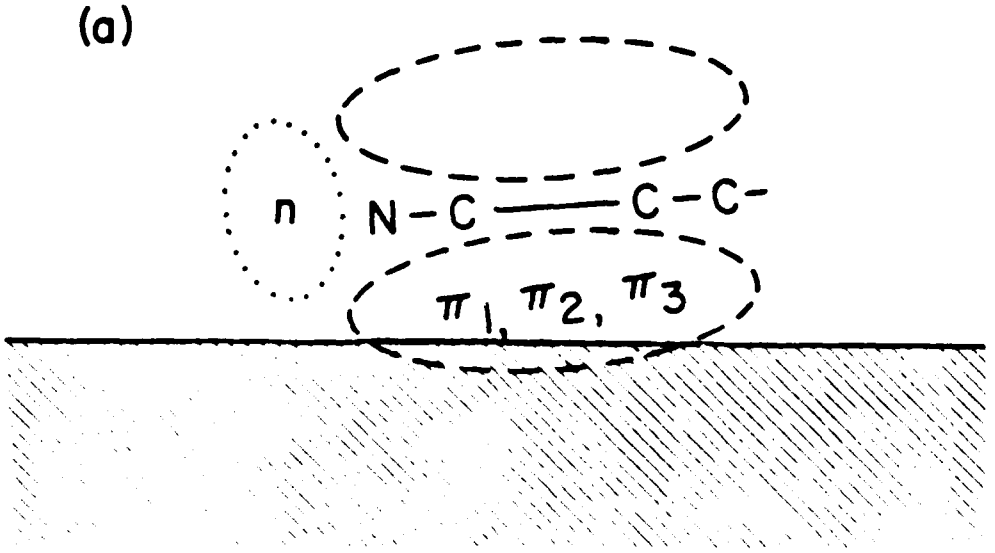

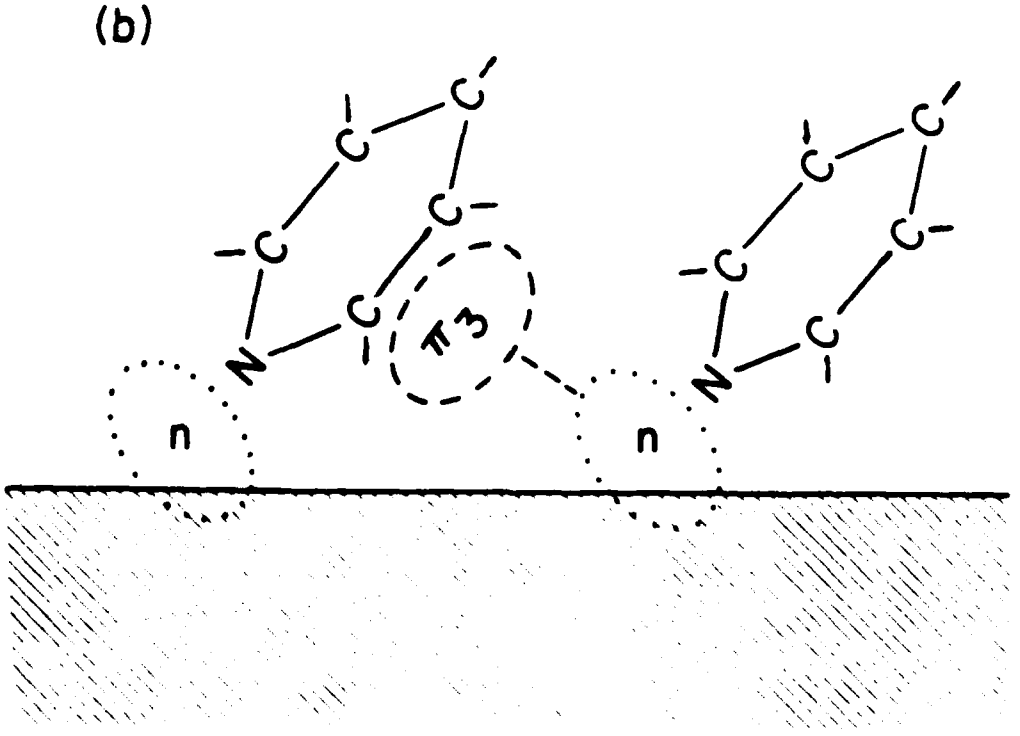

FIG 4
DEMUTH, ET, AL

TECHNICAL REPORT DISTRIBUTION LIST, GEN

	No. Copies
Office of Naval Research Attn: Code 472 800 North Quincy Street Arlington, Virginia 22217	2
ONR Branch Office Attn: Dr. George Sandoz 536 S. Clark Street Chicago, Illinois 60605	1
ONR Area Office Attn: Scientific Dept. 715 Broadway New York, New York 10003	1
ONR Western Regional Office 1030 East Green Street Pasadena, California 91106	1
ONR Eastern/Central Regional Office Attn: Dr. L. H. Peebles Building 114, Section D 666 Summer Street Boston, Massachusetts 02210	1
Director, Naval Research Laboratory Attn: Code 6100 Washington, D.C. 20390	1
The Assistant Secretary of the Navy (RE&S) Department of the Navy Room 4E736, Pentagon Washington, D.C. 20350	1
Commander, Naval Air Systems Command Attn: Code 310C (H. Rosenwasser) Department of the Navy Washington, D.C. 20360	1
Defense Technical Information Center Building 5, Cameron Station Alexandria, Virginia 22314	12
Dr. Fred Saalfeld Chemistry Division, Code 6100 Naval Research Laboratory Washington, D.C. 20375	1
U.S. Army Research Office Attn: CRD-AA-IP P.O. Box 1211 Research Triangle Park, N.C. 27709	1
Naval Ocean Systems Center Attn: Mr. Joe McCartney San Diego, California 92152	1
Naval Weapons Center Attn: Dr. A. B. Amster, Chemistry Division China Lake, California 93555	1
Naval Civil Engineering Laboratory Attn: Dr. R. W. Drisko Port Hueneme, California 93401	1
Department of Physics & Chemistry Naval Postgraduate School Monterey, California 93940	1
Dr. A. L. Slafkosky Scientific Advisor Commandant of the Marine Corps (Code RD-1) Washington, D.C. 20380	1
Office of Naval Research Attn: Dr. Richard S. Miller 800 N. Quincy Street Arlington, Virginia 22217	1
Naval Ship Research and Development Center Attn: Dr. G. Bosmajian, Applied Chemistry Division Annapolis, Maryland 21401	1
Naval Ocean Systems Center Attn: Dr. S. Yamamoto, Marine Sciences Division San Diego, California 91232	1
Mr. John Boyle Materials Branch Naval Ship Engineering Center Philadelphia, Pennsylvania 19112	1

TECHNICAL REPORT DISTRIBUTION LIST, GEN

	No. Copies
Dr. Rudolph J. Marcus Office of Naval Research Scientific Liaison Group American Embassy APO San Francisco 96503	1
Mr. James Kelley DTNSRDC Code 2803 Annapolis, Maryland 21402	1

TECHNICAL REPORT DISTRIBUTION LIST, 056

	No. Copies
Dr. D. A. Vroom IRT P.O. Box 80817 San Diego, California 92138	1
Dr. G. A. Somorjai Department of Chemistry University of California Berkeley, California 94720	1
Dr. L. N. Jarvis Surface Chemistry Division 4555 Overlook Avenue, S.W. Washington, D.C. 20375	1
Dr. J. B. Hudson Materials Division Rensselaer Polytechnic Institute Troy, New York 12181	1
Dr. John T. Yates Surface Chemistry Section National Bureau of Standards Department of Commerce Washington, D.C. 20234	1
Dr. Theodore E. Madey Surface Chemistry Section Department of Commerce National Bureau of Standards Washington, D.C. 20234	1
Dr. J. M. White Department of Chemistry University of Texas Austin, Texas 78712	1
Dr. Keith H. Johnson Department of Metallurgy and Materials Science Massachusetts Institute of Technology Cambridge, Massachusetts 02139	1
Dr. J. E. Demuth IBM Corporation Thomas J. Watson Research Center P.O. Box 218 Yorktown Heights, New York 10598	1
Dr. C. P. Flynn Department of Physics University of Illinois Urbana, Illinois 61801	1
Dr. W. Kohn Department of Physics University of California (San Diego) LaJolla, California 92037	1
Dr. R. L. Park Director, Center of Materials Research University of Maryland College Park, Maryland 20742	1
Dr. W. T. Peria Electrical Engineering Department University of Minnesota Minneapolis, Minnesota 55455	1
Dr. Narkis Tzoar City University of New York Convent Avenue at 138th Street New York, New York 10031	1
Dr. Chia-Wei Woo Department of Physics Northwestern University Evanston, Illinois 60201	1
Dr. D. C. Mattis Polytechnic Institute of New York 333 Jay Street Brooklyn, New York 11201	1
Dr. Robert M. Hexter Department of Chemistry University of Minnesota Minneapolis, Minnesota 55455	1
Dr. R. P. Van Duyne Chemistry Department Northwestern University Evanston, Illinois 60201	1

TECHNICAL REPORT DISTRIBUTION LIST, 056

	No. Copies
Dr. M. G. Lagally Department of Metallurgical and Mining Engineering University of Wisconsin Madison, Wisconsin 53706	1
Dr. Robert Gomer Department of Chemistry James Franck Institute 5640 Ellis Avenue Chicago, Illinois 60637	1
Dr. R. G. Wallis Department of Physics University of California, Irvine Irvine, California 92664	1
Dr. D. Ramaker Chemistry Department George Washington University Washington, D.C. 20052	1
Dr. P. Hansma Chemistry Department University of California, Santa Barbara Santa Barbara, California 93106	1
Dr. P. Hendra Chemistry Department Southhampton University England S09JNH	1
Professor P. Skell Chemistry Department Pennsylvania State University University Park, Pennsylvania 16802	1
Dr. J. C. Hemminger Chemistry Department University of California, Irvine Irvine, California 92717	1
Dr. Martin Fleischmann Department of Chemistry Southampton University Southampton 509 5NH Hampshire, England	1
Dr. J. Osteryoung Chemistry Department SUNY, Buffalo Buffalo, New York 14214	1
Dr. G. Rubloff I.B.M. Thomas J. Watson Research Center P. O. Box 218 Yorktown Heights, New York 10598	1
Dr. J. A. Gardner Department of Physics Oregon State University Corvallis, Oregon 97331	1
Dr. G. D. Stein Mechanical Engineering Department Northwestern University Evanston, Illinois 60201	1
Dr. K. G. Spears Chemistry Department Northwestern University Evanston, Illinois 60201	1
Dr. R. W. Plummer University of Pennsylvania Department of Physics Philadelphia, Pennsylvania 19104	1
Dr. E. Yeager Department of Chemistry Case Western Reserve University Cleveland, Ohio 41106	2
Professor George H. Morrison Cornell University Department of Chemistry Ithaca, New York 14853	1
Professor N. Winograd Pennsylvania State University Chemistry Department University Park, Pennsylvania 16802	1
Professor Thomas F. George The University of Rochester Chemistry Department Rochester, New York 14627	1